Journal of Engineering Science 10(1), 2019, 31–43

JES
an international Journal

STUDY THE IMPACT ON ENVIRONMENTAL MOISTURE DURING THE INTENSIFICATION AND MOVEMENT OF TROPICAL CYCLONE HUDHUD IN THE BAY OF BENGAL USING WRF-ARW MODEL

Sumon Kumar Das and M. M. Alam*

Department of Physics, Khulna University of Engineering & Technology, Khulna-9203, Bangladesh

Received: 10 March 2019 Accepted: 25 May 2019

ABSTRACT

Comprehensive sensitivity analysis on physical parameterization schemes of Advanced Weather Research and Forecasting model (ARW-WRF v3.8.1) has been carried out for the impact of environmental moisture on the intensification and movement of Tropical Cyclone (TC) Hudhud, which formed in the Bay of Bengal and crossed the eastern coast of India on 12 October 2014. The model was run by using WSM6-class graupel, Thomson graupel, WDM6-class graupel and NSSL mom-1 (NSSL-1) microphysics schemes (MPs) coupling with Kain-Fritsch (KF) cumulus parameterization (CP) scheme with four different initial conditions. The model was run for 168, 144, 120 and 96-h using the initial conditions at 0000 UTC of 6, 7, 8 and 9 October 2014. For the analysis of movement and impact of environmental moisture on TC we have selected two square area one at the front and another one at the rear position. In this research the front and rear positions of TC Hudhud are considered (17-20^{o}N & 85-88^{o}E) and (7-10^{o}N & 92-95^{o}E), respectively. Relative humidity (RH),wind speed (WS) and wind direction (WD) at different vertical levels have been analyzed in rear and front positions and time variation of water vapor mixing ratio (WVMR) have been studied at 2 meter level. The RH is found to increase continuously at front position as the cyclone Hudhud moves towards the front and decrease at rear position as it moves further from this selected area before crossing the land; after that it has decreased at front and increased at rear positions for all initial conditions of model run. The area average WS is found to increase (decrease) at front (rear) position from 950 to 250 (950 to 450) hPa for all MPs before crossing the land for all initial conditions of model run. Due to the northeasterly to easterly wind from surface to 200 hPa level during 8-10 October 2014 and southeasterly wind on 11 October at front position the TC Hudhud moved towards the eastern coast of India.

1. INTRODUCTION

Tropical cyclones (TC) are known to cause enormous damage and destruction in the coastal regions of Bangladesh. Strong winds at the center of the low abundance of moisture and latent heat, which brings the storm to supply the necessary energy. Although TC help to moderate climate by transferring energy from warm equatorial regions to cooler higher latitudes, the combined effects of their extreme wind, precipitation, and storm surge threaten the lives of millions of people who live near the coast. TC Hudhud caused extensive damage to the city of Visakhapatnam and the neighboring districts of Vizianagaram and Srikakulam of Andhra Pradesh. Damages were estimated to be US$3.58 billion by the Andhra state government of India. At least 124 deaths have been confirmed, a majority of them from Andhra Pradesh and Nepal, with the latter experiencing an avalanche due to the cyclone. Wu *et al.* (2015) studied on the impact of environmental moisture on TC intensification and found that the convection in the environment can have favorable impacts on the storm intensity. Emanuel *et al.* (2004) studied the environmental control of TC intensity. In their study, the model is used to explore the sensitivity of storm intensity to its initialization and to a number of environmental factors, including potential intensity, storm track, wind shear, upper-ocean thermal structure, bathymetry, and land surface characteristics. Environmental moisture has been considered as one of the important factors for TC intensity forecasting. As one of the skillful predictors, the 850 hPa relative humidity (RH) averaged between 200 and 800 km from storm center has been used routinely in the statistical hurricane intensity prediction scheme (SHIPS) for hurricane intensity forecasting at the National Hurricane Center (Kaplan *et al.,* 2010).

Hill and Lackmann (2009) studied on influence of environmental humidity on TC Size. They recommended that the size of TC controlled by the environmental factors. Tao and Zhang (2014) suggested that the development of TCs is largely depending on the magnitude of vertical wind shear and diabetic heating. Wu and Chen (2012) studied on the sensitivity of TC precipitation to atmospheric moisture content of Bilis. Their result suggested that the TC precipitation decreased dramatically with the reduction of ambient water vapor content in the atmosphere. Taraphdar *et al.* (2014) demonstrated that the moist convection plays a major role in intrinsic error growth, which limit the intrinsic predictability of the TC.

Frank and Ritchie (1998) studied the effects of environmental flow upon TC Structure. They recommended that the pattern of convection in the storm's core is strongly influenced by vertical wind shear and to comparable

* Corresponding Author: malam@phy.kuet.ac.bd

degree by boundary layer friction. Emanuel *et al.* (2004) and Kimball (2006) have suggested that the high environmental moisture may be conducive to TC intensification. Dry air intrusion could lead to a weakening of a TC by inducing asymmetric convective activity and transporting low equivalent potential temperature (θ_e) air into the sub-cloud layer and storm inflow (e.g., Braun *et al*., 2012; Emanuel, 1989; Ge *et al*., 2013). However, some studies (Wang *et al.*, 2009; Ying and Zhang, 2012) showed that substantial moisture may also cause a negative impact on TC strength by facilitating the formation of TC rain bands, which reduces the horizontal pressure gradient of a TC.

Alam (2014) has simulated the heavy rainfall events using 9 and 3 km nested domain from 7–9 October 2007 over Bangladesh. In this research, the sensitivity of six different microphysical schemes (Kessler, Lin *et al*., WSM3, Ferrier, WSM6 and Thompson) and two different cumulus parameterization schemes, Kain–Fritsch (KF) and Betts–Miller–Janjic (BMJ) were considered. Out of 12 combinations, the WSM6-KF has given better prediction and after that Lin-KF combination. WSM3-KF has simulated less area averaged rainfall out of all combinations. Hasan *et al.* (2018) studied the evaluation of microphysics and cumulus parameterization schemes of WRF for forecasting of heavy monsoon rainfall over the southeastern hilly region of Bangladesh. In this research it is found that WRF experiments with Stony Brook University (SBU) scheme along with Tiedtke (TD) cumulus scheme can produce best forecast for the heavy rainfall event of 2012 over the southeastern hilly regions of Bangladesh. The second best combination is using WRF single moment 6-class microphysics (WSM6) scheme and Grell (GR) cumulus scheme for a WRF experiment.

Das *et al.* (2015) studied the sensitivity of physical parameterization schemes for the simulation of mesoscale convective systems associated with squall events. This study shows that the prediction of parameters associated with squalls are sensitive to parameterization schemes of Milbrandt, YSU, KF and Grell-Devenyi ensemble scheme. The combination of Milbrandt, No CU, YSU schemes provides the best results as compared to all other combinations of parameterization schemes.

In the present study, the Weather Research and Forecast (WRF-ARWv3.8.1) model is used to simulate the environmental moisture at front and rear positions on tropical cyclone intensification over the Bay of Bengal. The objective of this research is to investigate the average moisture propagated in different vertical levels through the front and rear positions of TC Hudhud. Attempt has been made to identify the changing pattern of Relative humidity (RH), wind speed (WS) and wind direction (WD) at different vertical levels in rear and front positions and time variation of water vapor mixing ratio (WVMR) at 2 meter levels have been studied on TCs movements and intensification in the Bay of Bengal.

2. MODEL DESCRIPTION

The model is configured in single domain (Figure 1), 9 km horizontal grid spacing with 291×317 grids in the west-east and north-south directions and 19 vertical levels. The four different microphysics used for sensitivity study are WSM 6-class, Thompson, WDM6 and NSSL-1 schemes. To examine the impact of TC on moisture in the troposphere, we have used those schemes for the simulation of TC Hudhud. The cumulus parameterization (CP) scheme used in WRF model is Kain-Fritsch (KF). The detailed configuration of WRF model Physics, dynamics and model domain is given in Table 1.

Figure 1: The WRF–ARW domain set up for the study.

Table 1: WRF Model and Domain Configurations

Dynamics	Non-hydrostatic
Horizontal grid distance	9 km
Integration time step	45 s
Number of grid points	X-direction 291 points, Y-direction 317 points
Map projection	Mercator
Vertical co-ordinate	Terrain-following hydrostatic-pressure co-ordinate (19 sigma levels up to 100 hPa)
Microphysics	1) WSM6, (2) Thompson, (3) WDM6 and (4) NSSL-1 scheme.
Radiation scheme	Dudhia for short wave radiation/ RRTM long wave Mlawer *et al.* (1997)
Surface layer	Monin– Obukhov similarity theory scheme
Land surface parameterization	5 Layer Thermal diffusion scheme (Ek *et al.,* 2003)
Cumulus parameterization schemes	Kain-Fritsch scheme (KF)
PBL parameterization	Yonsei University Scheme (YSU) scheme

The details of microphysical and cumulus parameterization schemes are given below:

WSM6 scheme: The WRF-single-moment-6-class (WSM6) microphysics scheme predicts the mixing ratios for water vapor, cloud water, cloud ice, snow, rain, and graupel. A new method for representing mixed-phase particle fall speeds for the snow and graupel by assigning a single fall speed to both that is weighted by the mixing ratios, and applying that fall speed to both sedimentation and accumulation processes is introduced (Dudhia *et al.,* 2008) of the three WSM schemes. Of the three WSM schemes, the WSM6 scheme is the most suitable for cloud resolving grids, considering the efficiency and theoretical backgrounds (Hong *et al.,* 2006). The WSM6 scheme has been developed by adding additional process related to graupel to the WSM6 scheme (Hong and Lim, 2006).

Thompson *et al.* scheme: A bulk microphysical parameterization (BMP) developed for use with WRF or other mesoscale models. The snow size distribution depends on both ice water content and temperature and is represented as a sum of exponential and gamma distributions. Furthermore, snow assumes a non-spherical shape with a bulk density that varies inversely with diameter as found in observations. A new scheme with ice, snow and graupel processes suitable for high-resolution simulations Thompson *et al.,* (2007).

WDM6 Scheme: The WRF double-moment 6-class (WDM6) microphysics scheme implements a double moment bulk microphysical parameterization of clouds and precipitation and is applicable in mesoscale and general circulation models. The WDM6 scheme enables the investigation of the aerosol effects on cloud properties and precipitation processes with the prognostic variables of cloud condensation nuclei (CCN), cloud water and rain number concentrations. WDM6 extends the WSM6 by incorporating the number concentrations for cloud and rainwater along with a prognostic variable of CCN number concentration. Moreover, it predicts the mixing ratios of six water species (water vapor, cloud droplets, cloud ice, snow, rain, and graupel), similar to WSM6. Prognostic water substance variables include water vapor, clouds, rain, ice, snow, and graupel for both the WDM6 and WSM6 schemes. Additionally, the prognostic number concentrations of cloud and rain waters, together with the CCN, are considered in the WDM6 scheme. The number concentrations of ice species such as graupel, snow, and ice are diagnosed following the ice-phase microphysics of Hong *et al.* (2004).

NSSL-1 Moment Scheme: The NSSL-1 moment predicts the mass mixing ratio and number concentration for six hydrometeor species: cloud droplets, rain drops, ice crystals, snow, graupel and hail (Mansell *et al.,* 2010). A unique feature is the additional prediction of average graupel particle density, which allows graupel to span the range from frozen drops to low-density graupel. Hail is produced only by wet growth of graupel to try to represent true hail rather than merely high-density ice. An option allows prediction of CCN concentration. The scheme also features adaptive sedimentation to allow some size sorting but prevent spurious large particles that can arise from one-moment microphysics, particularly for the larger precipitation categories.

Kain–Fritsch (KF) scheme: In the KF scheme, the condensates in the updraft are converted into precipitation when their amount exceeds threshold value. In this scheme, the convection consumes the convective available potential energy (CAPE) in a certain time scale. The KF scheme also includes the shallow convection other than deep convection. The shallow convection creates non-perceptible condensates and the shallowness of the convection is determined by a vertical extent of the cloud layer that is known by a function of temperature at Lifting Condensation Level (LCL) of rising air parcel (Kain *et al*., 1990). In this scheme updraft generates condensate and dump condensate into environment downdraft evaporates condensate at a rate that depends on RH and depth of downdraft leftover condensate accumulates at surface as precipitation.

3. DATA AND METHODOLOGY

Final Reanalysis (FNL) data (1^o x1^o) collected from National Centre for Environment Prediction (NCEP) is used as initial and lateral boundary conditions (LBCs) which is updated at six hours interval i.e. the model is initialized with 0000, 0600, 1200 and 1800 UTC initial fields of corresponding date. The NCEP FNL data is interpolated to the model horizontal and vertical grids and the model was integrated for 168, 144, 120 and 96-h period for TC Hudhud. 16 experiments have been conducted by using WSM6, Thompson, WDM6 and NSSL-1 schemes in combinations with KF scheme with four different initial conditions. In this regard, the initial conditions of 0000 UTC of 6-9 October 2014 for TC Hudhud are used.

The model simulated WVMR, RH, WS and WD have been analyzed. Simulated track and intensity have been compared with the observed results of Indian Meteorological Department (IMD). In this research, two different regions have been considered inside the model domain one at front position (17-20^o N & 85-88^o E) and another at rear position (7-10^o N & 92-95^o E). We have tried to identify, how changes are observed in the analyzed parameters at front and rear positions and what are the impact on the intensification of TC of these changes at these positions. After getting text data from Grid Analysis and Display System (GrADS), it converted into Excel sheet and plotted graph using Excel.

Table 2: Observed information of TC Hudhud in the Bay of Bengal

Name of TC	Place of landfall	Date of Formation	Date and Time of landfall, UTC	Minimum SLP, hPa	Maximum Sustained Wind Speed, m/s
Hudhud	Visakhapatnam, India	7 October	0630 and 0730 UTC of 12 October 2014	950	51

4 RESULTS AND DISCUSSION

The water vapor mixing ratio (WVMR) at 2 m level, relative humidity (RH),wind speed and wind direction at different vertical levels at front and rear positions, track and intensity in whole domain have been simulated and analyzed during the formation, intensification and movement of TC Hudhud. The results of these parameters have been presented and discussed in the following sub-sections.

4.1 Track of TC Hudhud

The tracks model runs for 168, 144, 120 and 96-h with the initial conditions at 0000 UTC of 6-9 October 2014 for WSM6, Thompson, WDM6 and NSSL mom-1 microphysics schemes and IMD observed track are presented as in Figures 2(a-d). The track deviated most from IMD observed track by Thomson and NSSL mom-1 schemes with the initial conditions of 6 (Figure 2a), 7 (Figure 2b) and 8 (Figure 2c) October model run.

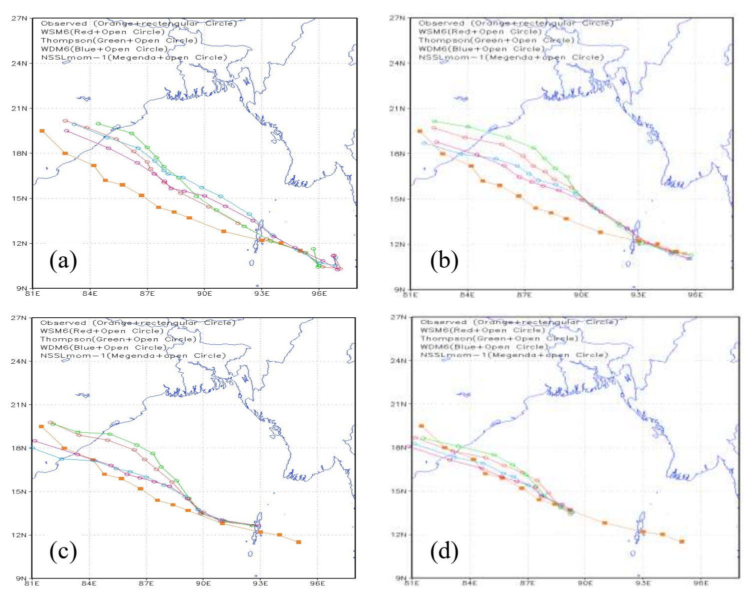

Figure 2: IMD observed and Model simulated tracks of TC Hudhud using four different MP schemes coupled with KF scheme with the initial conditions at 0000 UTC of (a-d) 6-9 October, respectively.

As the initial conditions of model run proceeds towards the landfall time the position of all tracks moved from right towards left i.e. towards the actual landfall position. The landfall time were 0600, 1100 UTC of 11 October and 1800 and 1800 UTC of 12 October for Thompson, WSM6, NSSL and WDM6 schemes, respectively. The track deviation at the time of landfall is less for all MPs schemes with the initial conditions at 0000 UTC of 9 October (Figure 2d) and landfall times for WSM6, Thompson, WDM6 and NSSL schemes are 1100, 0500, 1800, 1800 UTC of 12 October. WSM6 scheme gives the better results for the initial conditions at 0000 UTC of 6 (figure not shown) and 8 October and WSM6 and NSSL mom-1 schemes gives the better results for the initial conditions at 8 and 9 October. Due to the northeasterly to easterly flow during 8-10 October and southeasterly flow on 11 October the TC Hudhud moved towards west northwestern direction and crossed Visakhapatnam coast of India. The average error of track was found for WSM6, Thompson, WDM6 and NSSL schemes are 175, 217, 217 and 213; 173, 209, 155 and 162; 140, 163, 83 and 103; and 86, 95, 74 and 83 km for the initial conditions of 6-9 October, respectively. The average track error was found minimum for WDM6 schemes with the initial conditions at 7-9 October, which suggest the better performance among the MPs.

4.2 Intensity of TC Hudhud

The observed MSLP was 950 hPa and Thompson, WSM6, NSSL and WDM6 schemes of WRF model have simulated 909, 922, 927 and 938 hPa (Figure 3a) for the initial conditions at 0000 UTC of 9 October, respectively. The similar pattern of MSLP is also found for all MPs with all other initial conditions of 0000 UTC of 6, 7 and 8 October (Figure not shown). The model simulated pressure for different MPs with different initial conditions are much lower than that of IMD estimated pressure (950 hPa). For all initial conditions of model run Thompson and WDM6 schemes have simulated highest and lowest pressure fall, but the pressure fall by WDM6 scheme is closer to the IMD observed pressure. The MSLP has simulated 922 and 944 hPa at 1800 UTC of 11 October and 955 and 909 hPa (Figure 3b) at 0000 of 12 October at front position for WSM6, WDM6 NSSL and Thompson schemes, respectively for the initial conditions at 0000 UTC of 9 October. The simulated MSLP at front position by WDM6 and NSSL schemes are closer to the IMD estimated MSLP and time of MSLP (950hPa at 0600 UTC of 12 October). There is almost no change of MSLP at rear position for all MP schemes with all initial conditions of model run (Figure 3c).

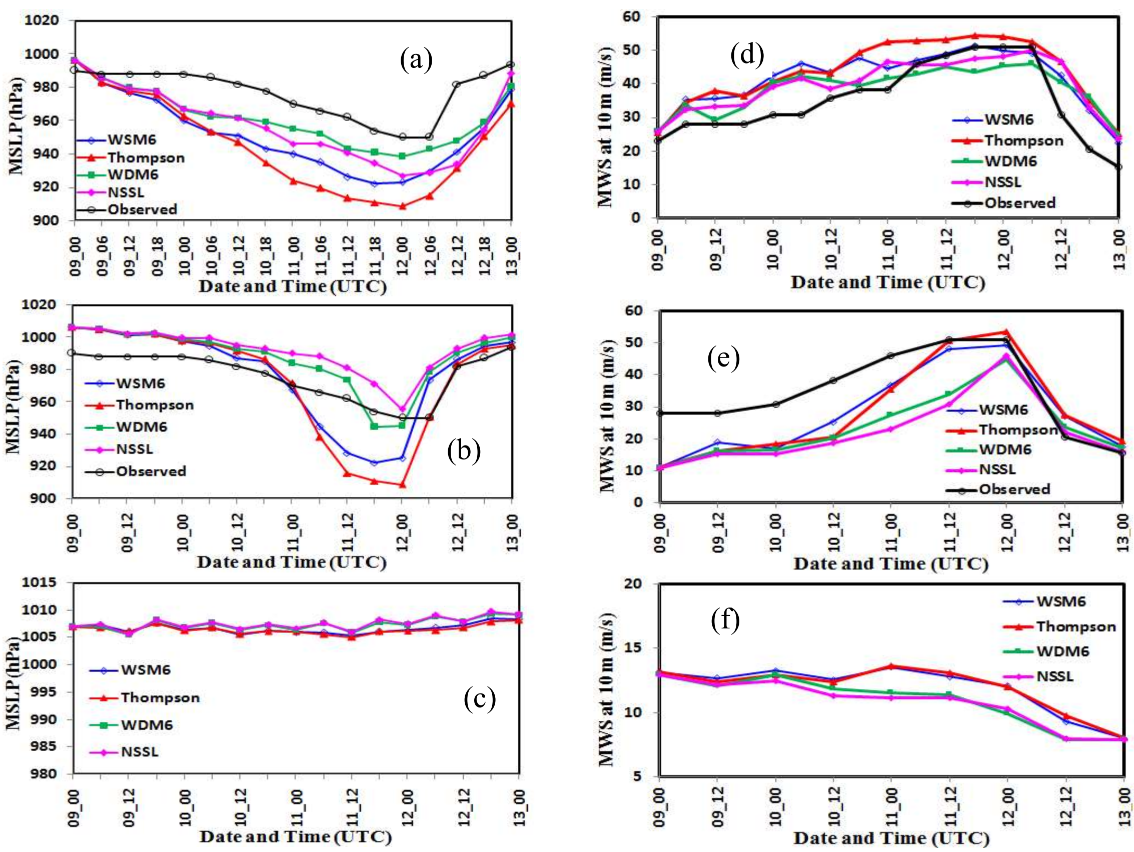

Figure 3: Model simulated (a-c) MSLP and (d-f) MWS at 10 m level at whole domain, front and rear positions of TC Hudhud using four different MP schemes with the initial conditions at 0000 UTC of 9 October respectively.

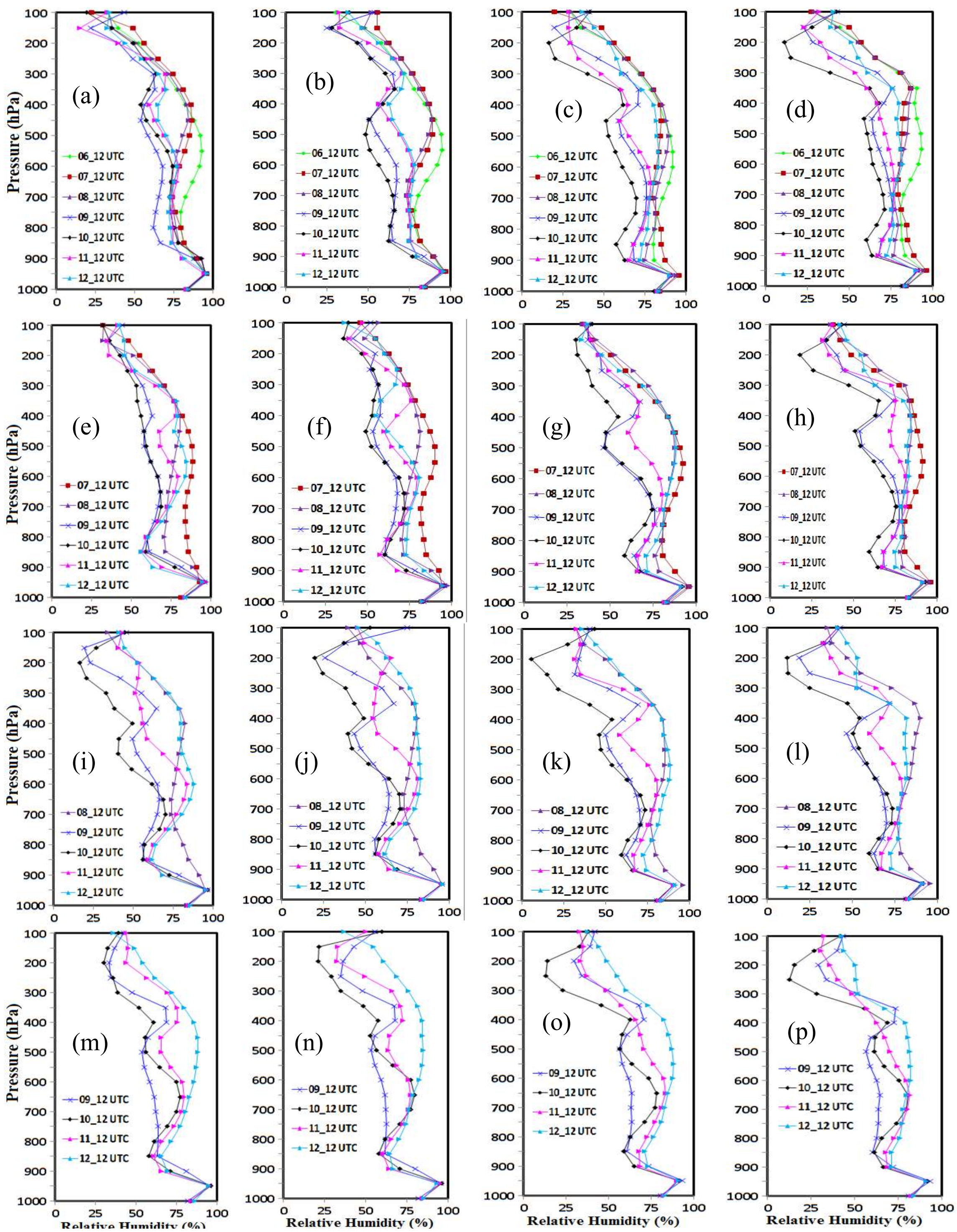

Figure 4: Model simulated area averaged RH (%) at 1200 UTC of different days in front of TC Hudhud for WSM6, Thompson, WDM6 and NSSL-1 schemes at 0000 UTC of (a-d) 6, (e-h) 7, (i-l) 8 and (m-p) 9 October 2014 initial conditions respectively.

The simulated MWS were 54, 51, 50 and 46 m s^{-1} at 1800 UTC of 11 October for Thompson and WSM6 schemes, and 0600 UTC of 12 October for NSSL and WDM6 schemes, respectively (Figure 3d). The model simulated MWSs for different MPs with different initial conditions are almost similar to that of IMD observed MWS (51 m s^{-1} at 0600 UTC of 12 October). The simulated MWS at front position were 45, 46, 49 and 54 m s^{-1} at 0000, 1200, 0000 UTC of 11 and 0000 UTC of 12 October for WDM6, NSSL, WSM6 and Thompson schemes (Figure 3e), respectively for the initial conditions of 0000 UTC of 9 October. The MWS for WDM6, NSSL, WSM6 schemes were reached maximum after front position. At the rear position the MWS at 10m level is found to decrease continuously as the TC moved further from the rear position (Figure 3f).

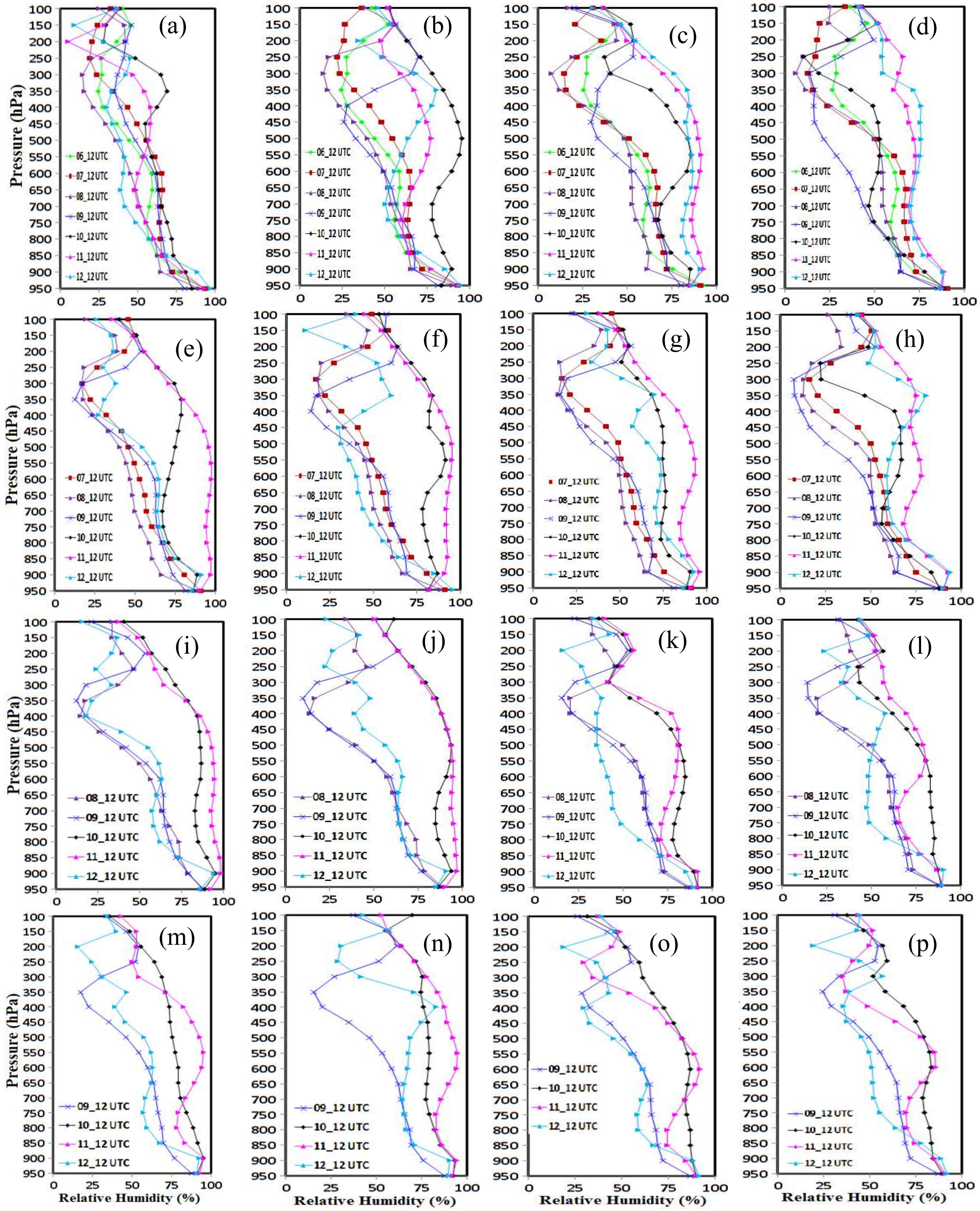

Figure 5: Model simulated area averaged RH (%) at 1200 UTC of different days in rear of TC Hudhud for WSM6, Thompson, WDM6 and NSSL-1 schemes at 0000 UTC of (a-d) 6, (e-h) 7, (i-l) 8 and (m-p) 9 October 2014 initial conditions respectively.

4.3 Relative Humidity (RH)

Model simulated vertical profiles of area averaged RH (%) at front position with four different MPs coupling with KF scheme are presented in figure 4 for 0000 UTC of 6-9 October 2014 initial conditions. The simulated RH is below 90% for all MPs from surface to 100 hPa levels for the initial conditions at 0000 UTC of 6-9

October. From Figure 4, it is seen that the simulated RH is minimum in the upper troposphere at around 400-100 hPa. The distribution pattern of RH at 0000 UTC and 1200 UTC are almost similar so that only 1200 UTC graphs are presented in this research. The vertical variation of area average RH shows the increasing pattern for WSM6, Thompson, WDM6 and NSSL-1 schemes [Figures 4(a-d)] during 6-7 October and 9-11 October for the initial conditions of 0000 UTC of 6 October.

The vertical variation of area average RH is found to increase throughout the troposphere for all MPs during 8-11 October [Figures 4(e-h)], 9-11 October [Figures 4(i-l)] and 9-11 October [Figures 4(m-p)] for the initial conditions of 0000 UTC of 7-9 October respectively. The RH is found to decrease on 12 October i.e. after crossing the land on 12 October with little exception for all initial conditions of model run i.e. 0000 UTC of 6-9 October. Vertical variations of area averaged RH (%) at rear position with four different MPs coupling with KF scheme for the initial conditions at 0000 UTC of 6-9 October 2014 are presented in Figures 5(a-p). The area average RH is found to decrease [Figures 5(a-d)] throughout the troposphere for WSM6, Thompson, WDM6 and NSSL schemes during 6-10 October and increase on 11-12 October with little exception for the initial conditions of 0000 UTC of 6 October.

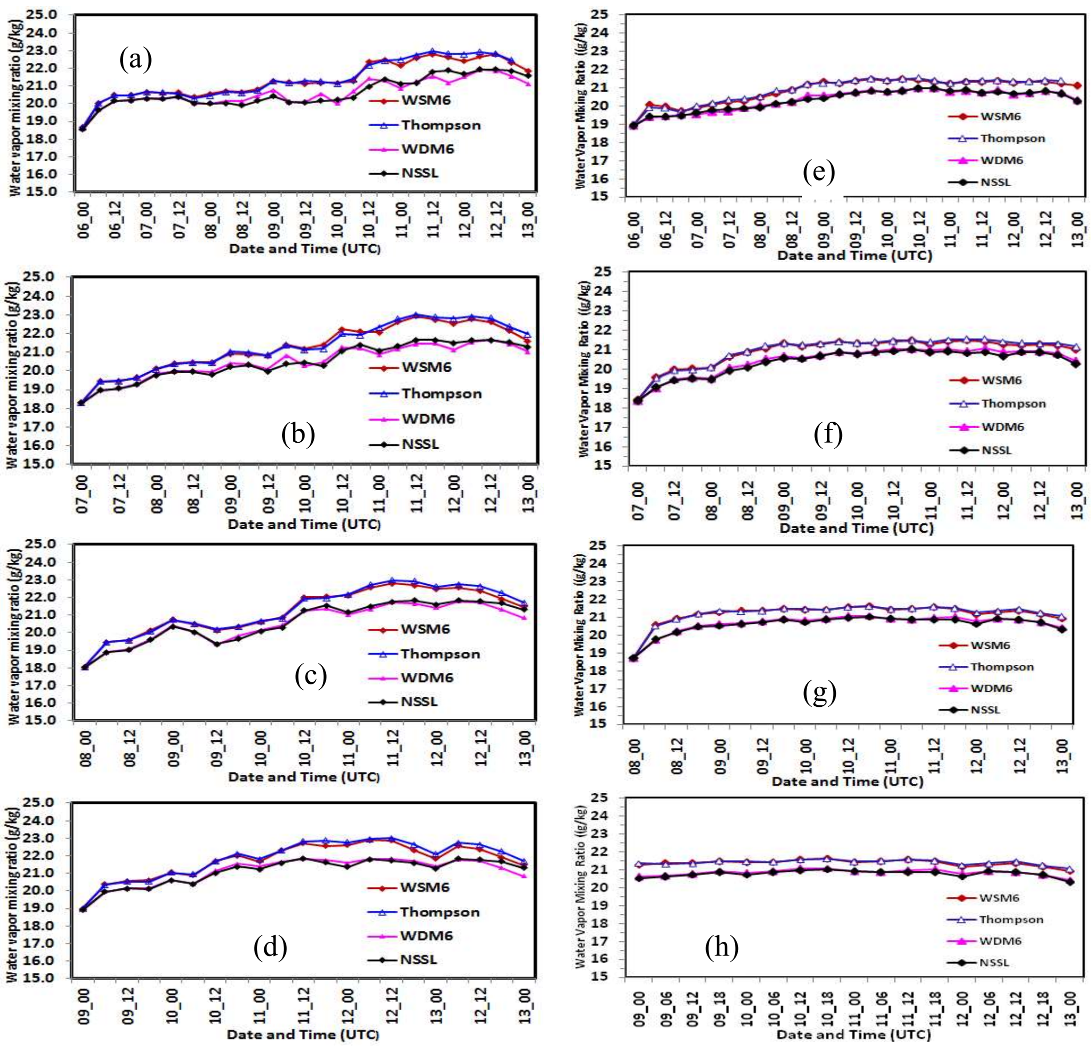

Figure 6: Model simulated area average WVMR of TC Hudhud for four different MPs in (a-d) front and (e-h) rear position at 0000 UTC of 6 - 9 October initial conditions respectively.

The area average RH is found to decrease throughout the troposphere for all MPs during 7-10 October [Figures 5(e-h)] and 8-10 October [Figures 5(i-l)] for the initial conditions of 0000 UTC of 7 and 8 October respectively. After that the RH is found to increase till 12 October i.e. after crossing the land with little exception. The area average RH is found to increase for all MP schemes during 9-12 October [Figures 5(m-p)] for the initial conditions of 0000 UTC of 9 October. The area average RH is found to increase at front position due to the movement of TC Hudhud towards this domain and decrease at rear position due to the further movement of TC from this domain from the starting of model run to 11 October and after that it has increased at rear position and decreased at front position. The RH increased in the front position favors intensification by providing more moisture to the inner core and promoting storm symmetry, with primary contributions coming from moisture increase in the boundary layer. There is impact of TC on RH with respect to intensification and movement.

4.2 Water Vapor Mixing Ratio (WVMR)

The temporal distribution of area average WVMR at 2 m level in front position for different MPs coupling with KF scheme of TC Hudhud is presented in Figures 6(a-h) for 0000 UTC of 6 - 9 October 2014 initial conditions. The area average WVMR at front position [Figures 6(a-d)] and rear position [Figures 6(e-h)] are found maximum for Thompson and minimum for WDM6 schemes using the initial conditions at 0000 UTC of 6 - 9 October 2014. The simulated area average WVMR at front position (Figure 6a) for different MPs are almost constant during 0000 UTC of 6-10 October and then it has increased and reached maximum at 1200 UTC of 11 October for the initial conditions of 0000 UTC of 6 October.

The area average WVMR is found maximum 22.8 g/kg and minimum 21.8 g/kg for Thompson and WDM6 schemes respectively. For the initial conditions of 0000 UTC of 7 October (Figure 6b), the temporal distribution of area average WVMR has increased continuously with the progression of time for all MPs and reached maximum at 1200 UTC of 11 October for different MPs respectively. The area average maximum and minimum WVMR are found to be 23 and 21.4 g/kg for Thompson and WDM6 schemes respectively. The temporal distribution of area average WVMR for all MPs (Figure 6c) has increasing tendency except at 0000 to 1200 UTC of 9 October and reached maximum at 1200 UTC of 11 October for different MPs for the initial conditions at 0000 UTC of 8 October. The area average maximum and minimum WVMR are 23 and 21.7 g/kg for Thompson and WDM6 schemes respectively. For the initial conditions at 0000 UTC of 9 October, the area average WVMR at front position (Figure 6d) has increased for all MPs and reached maximum at 0600 UTC of 12 October for different MPs with little exception. The area average maximum and minimum WVMR are 23 and 21.8 g/kg for Thompson and NSSL-1 schemes respectively.

The area average WVMR at rear position for all MPs has increased and reached maximum (Figure 6e) at 1800 UTC of 9 October for WSM6 and WDM6 schemes and 1200 and 1800 UTC of 10 October for Thompson and NSSL-1 schemes respectively for the initial conditions at 0000 UTC of 6 October. For the initial conditions of 0000 UTC of 7 (Figure 6f) and 8 (Figure 6g) October, the area average WVMR for all MPs has increased up to 0000 UTC of 9 October and after that it is found almost constant. The area average maximum and minimum WVMR are 21.5 and 21 g/kg and 21.6 and 21 g/kg for Thompson and NSSL-1 schemes based on the initial conditions on 7 and 8 October respectively. The area average WVMR (Figure 6h) is found to increase till 1200 UTC of 9 October and after that it is found almost constant for all MPs for the initial conditions of 0000 UTC of 9 October. The maximum and minimum WVMR are 22 and 21 g/kg for Thompson and WDM6 schemes. It is found that the WVMR is increased as the cyclone moves towards the front position, which suggests that the cyclone moves in a direction where the WVMR has increased.

4.3 Wind Speed (WS) at different pressure levels

The vertical distribution of area average WS at front and rear positions of TC Hudhud have simulated with the initial conditions at 0000 UTC of 6-9 October 2014 using four different MPs. The distribution pattern of WS is almost similar at 0000 UTC and 1200 UTC so that only 1200 UTC graphs are presented. The area average WS has increased from 950 to 250 hPa significantly during 8-11 October for the initial conditions of 0000 UTC of 6 and 7 (Figure not shown) and 8 [Figures 7(a-d)] October and during 9-11 October for the initial conditions at 0000 UTC of 9 October [Figures 7(e-h)] as the cyclone moves towards the front position and it decreased on 12 October except NSSL-1 scheme. On 11 October, the WS is found significantly higher at 850 hPa for WSM6, Thompson and WDM6 schemes for the initial conditions at 0000 UTC of 6-8 October. The area average WS is almost constant from surface to 200 hPa level at front position for all initial conditions of model run, this suggest that the cyclonic circulation exists up to 200 hPa level. Irregular pattern of wind is found at 200-100 hPa level. The area average WS at rear position is found to increase for WSM6, Thompson, WDM6 and NSSL-1 schemes up to 8 October and decreased during 9-12 October for the initial conditions at 0000 UTC of 6 and 7 (Figure not shown), 8 [Figures 8(a-d)] and 9 [Figures 8(e-h)] October. The area average WS is found maximum at 850 hPa level and minimum at 400 hPa at rear position for all MPs for all different initial conditions.

The area average WS is found to increase continuously at front position from 950 to 250 hPa levels for all MPs as the cyclone moves towards or nearby the front position and after crossing over land the WS is found to decrease on 1200 UTC of 12 October for all initial conditions. The area average WS is found to decrease at rear position from 950 to 450 hPa levels for all MPs during 8 to 12 October for all initial conditions. The average WS is found to increase continuously at front area indicates more evaporation, which destabilizes the boundary layer and can trigger deep convection (Larissa and Christopher, 2005).

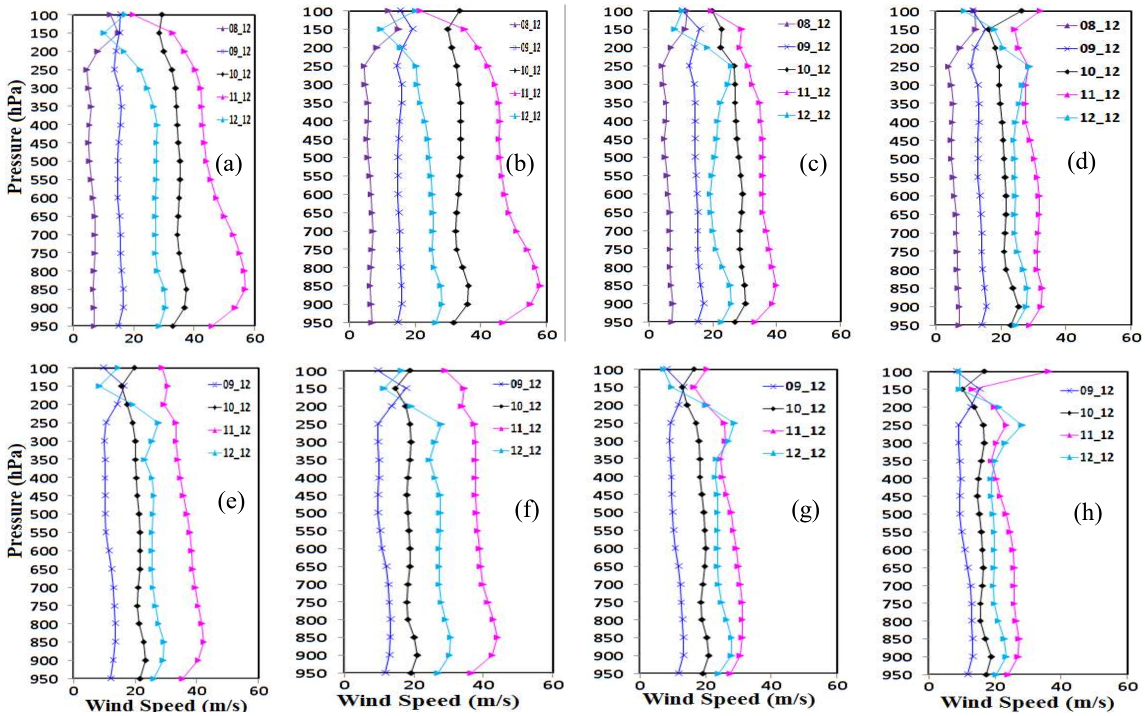

Figure 7: Model simulated area average wind speed at front position of TC Hudhud for WSM6, Thompson, WDM6 and NSSL-1 schemes at 0000 UTC of (a-d) 8 and (e-h) 9 October 2014 initial conditions respectively.

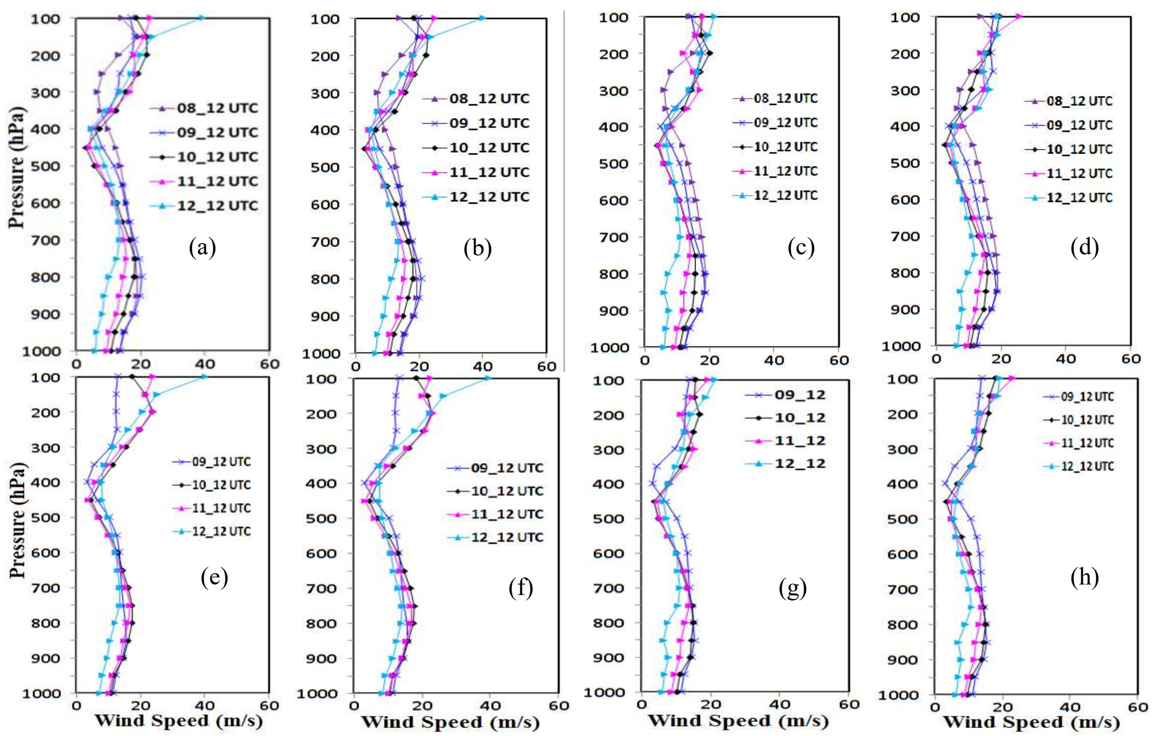

Figure 8: Model simulated area average WS at rear position of TC Hudhud for WSM6, Thompson, WDM6 and NSSL-1 schemes at 0000 UTC of (a-d) 8 and (e-h) 9 October 2014 initial conditions respectively.

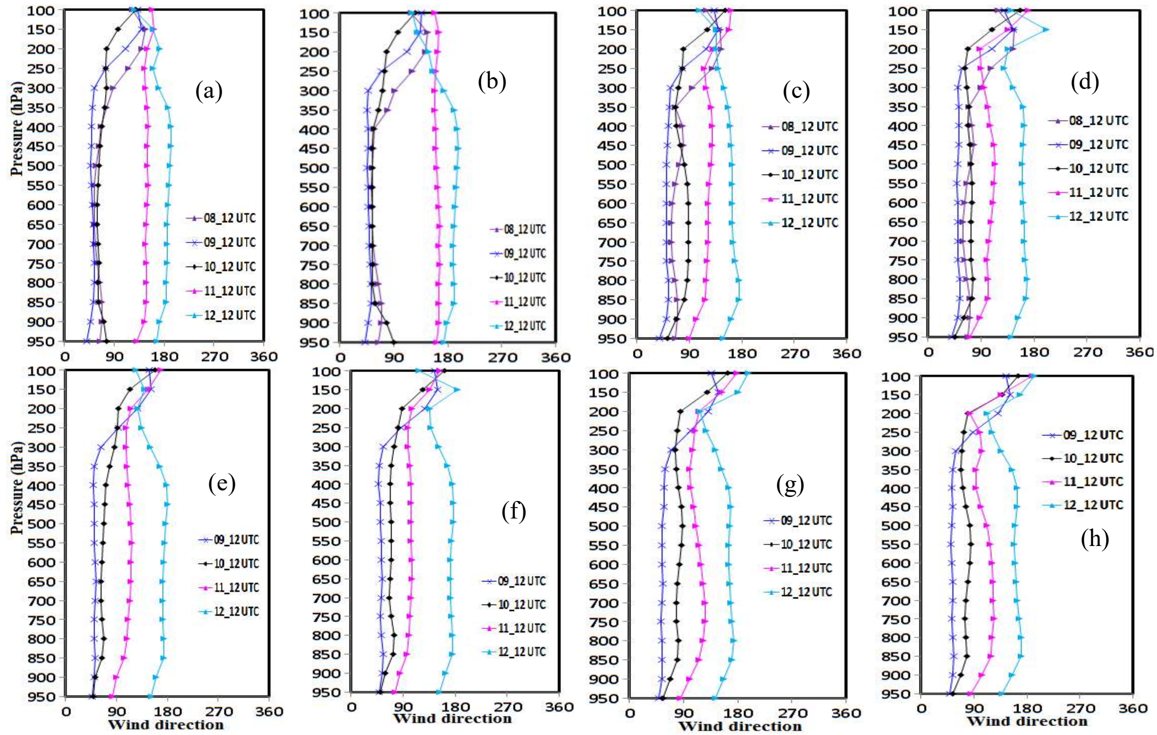

Figure 9: Model simulated area average WD at 1200 UTC of different days at front position of TC Hudhud for WSM6, Thompson, WDM6 and NSSL-1 schemes at 0000 UTC of (a-d) 8 and (e-h) 9 October 2014 initial conditions respectively.

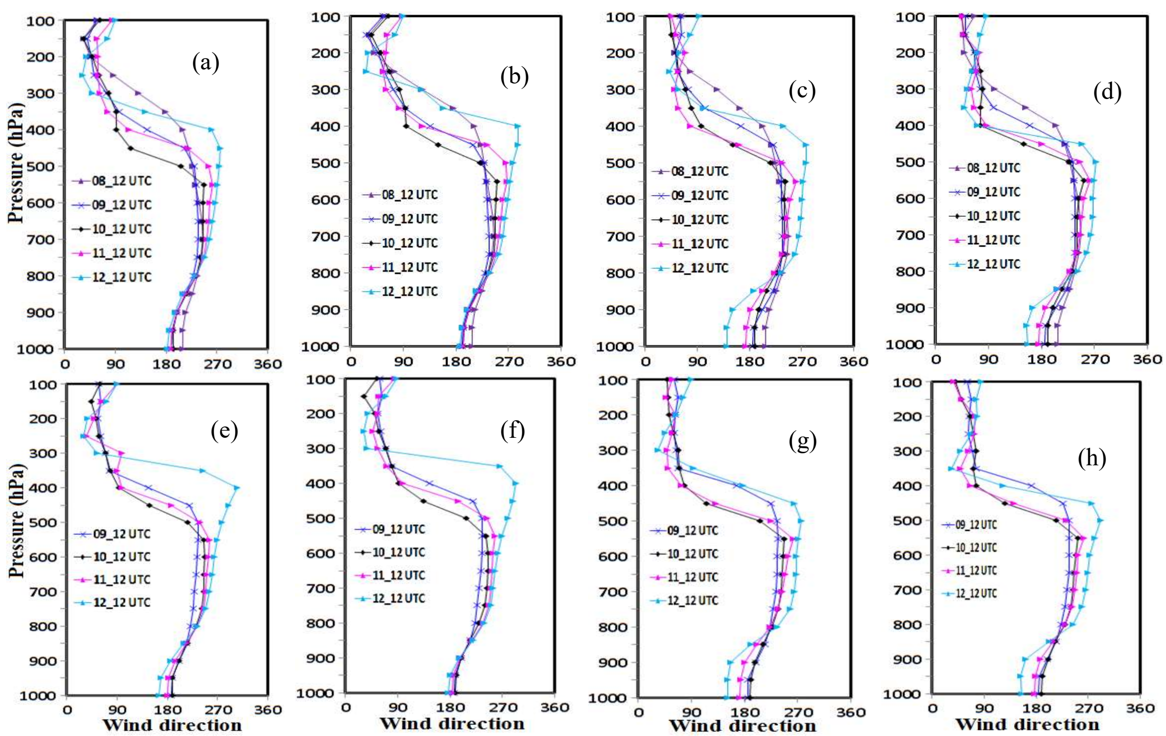

Figure 10: Model simulated area average WD at 1200 UTC of different days in rear position of TC Hudhud for WSM6, Thompson, WDM6 and NSSL-1 schemes at 0000 UTC of (a-d) 8 and (e-h) 9 October 2014 initial conditions respectively.

Physically, higher WS promote more evaporation, which destabilizes the boundary layer and can elicit deep convection. The WS increased continuously suggested more moisture at front position, which trigger deep convection. The WS has decreased continuously during 9-12 October suggested less moisture at rear position, which destabilizes the convection processes.

4.4 Wind Direction (WD)

Model simulated vertical variations of area average WD at front position for four different MPs are presented in Figures 9(a-h) for the initial conditions at 0000 UTC of 8 and 9 October 2014. The distribution pattern of WD for all MPs with different initial conditions at 0000 UTC and 1200 UTC are almost similar so that only the graphs at 1200 UTC are presented. It is observed from the simulated results that the easterly wind is flowing from surface to 600 hPa levels and westerly winds from 500 to 250 hPa levels on 6-7 October 2014 (Fig. not shown) for all MPs except NSSL-1 scheme with the initial conditions at 0000 UTC of 6 October. It is observed from the simulated results that the easterly wind is flowing from surface to 600 hPa levels and southerly to southwesterly winds from 500 to 250 hPa on 6 and 7 October 2014 (Fig. not shown) for all MPs with the 0000 UTC of 6 and 7 October initial conditions respectively.

During 8-10 October, the northeasterly to easterly wind flow is continuing and during 11-12 October the wind flow is shifted from northeasterly to south-southeasterly from surface to 100 hPa levels for all MPs with the 0000 UTC of 6 October initial conditions. Due to the northeasterly to easterly flow during 8-10 October at front position the TC moved towards west-southwestward i.e. the eastern coast of India and due to the southerly flow from surface to 100 hPa levels on 11 October, the TC shifted towards north and crossed eastern coast of Indian. The northeasterly wind is flowing from surface to 200 hPa levels on 8-10 [Figures 9(a-d)] and 9-10 [Figures 9(e-h)] October 2014 for all MPs with the initial conditions at 0000 UTC of 8 and 9 October, respectively. On 11 and 12 October, the south-southeasterly wind is flowing from surface to 200 hPa levels for all MPs with the 8 and 9 October 0000 UTC initial conditions. Due to the northeasterly to easterly flow during 8-10 October and southeasterly flow on 11 October, the TC Hudhud moved towards west northwestern direction and crossed Visakhapatnam coast of India. It is observed from the model simulated results that at rear position the area average wind is flowing southerly from surface to 850 hPa, westerly to southwesterly from 800 to 450 hPa and east-northeasterly wind from 450 to 100 hPa levels for all MPs for the initial conditions at 0000 UTC of 6 and 7 (Figure not shown), 8 [Figures 10(a-d)] and 9 [Figures 10(e-h)] October 2014.

5. CONCLUSIONS

From the present study, the following conclusions can be drawn:

- The RH is found to increase at front position and decrease at rear position from the starting of model run to 11 October i.e. before landfall and after that it has increased at rear position and decreased at front position. The RH and WVMR are found to increase in the direction in which the TC moves. The RH increased in the front position favors intensification by providing more moisture to the inner core and promoting storm symmetry.
- The area average WS is found to increase (decrease) at front (rear) positions from 950 to 250 (950 to 450) hPa levels for all MPs before crossing the land and after crossing it is found to decrease (increase) for all initial conditions of model run. Due to the northeasterly to easterly wind from surface to 200 hPa level during 8-10 October 2014 and southeasterly wind on 11 October at front position the TC Hudhud moved towards west i.e. eastern coast of India. In terms of intensity (pressure fall and MWS) the WDM6scheme shows better result out of all MPs and in terms of landfall time Thompson scheme gives the better results.
- The WS increased continuously suggested more moisture at front position, which trigger deep convection and decreased continuously during 9-12 October suggested less moisture at rear position, which destabilizes the convection processes.
- The area average WS is almost constant from surface to 200 hPa level at front position for all initial conditions of model run, this suggest that the cyclonic circulation exists up to 200 hPa level.
- The average track error was found minimum for WDM6 schemes with the initial conditions at 7-9 October, which suggest that, the WDM6 gives the better performance among all other used MPs.

ACKNOWLEDGEMENT

The authors are thankful to the Director of Bangladesh Meteorological Department (BMD) for providing the relevant data of this study. The authors gratefully acknowledge the NCEP/NCAR for providing WRF-ARW modeling system and their reanalysis data sets. The Grid Analysis and Display System (GrADS), Excel software were used for analytical purposes and displaying figures.

REFERENCES

Alam, M. M., 2014. Impact of cloud microphysics and cumulus parameterization on simulation of heavy rainfall event during 7-9 October 2007 over Bangladesh, *J. Earth Syst. Sci.* 123, 2, 259–279.

Braun, S. A., Sippel J. A., and Nolan D. S., 2012. The Impact of Dry Midlevel Air on Hurricane Intensity in Idealized Simulations with No Mean Flow, *J. Atmos. Sci.,* 69, 236–257, doi:10.1175/JASD-10-05007.1.

Das, M. K., Chowdhury M. A. M., and Das S., 2015. Sensitivity Study with Physical Parameterization Schemes for Simulation of Mesoscale Convective Systems Associated with Squall Events. International Journal of Earth and *Atmospheric Science*, 2(2), 20-36.

Dudhia, J., S.Y. Hong and K. S. Lim., 2008. A new method for representing mixed phase particle fall speeds in bulk microphysics parameterizations. *J. Met., Soc. Japan* vol. 86, 33-44.

Ek, M. A. A., Mitchell K. E., Lin Y., Rogers, Grundmann P., Koren V., Gayno G., and Tarpley J. D., 2003. Implementation of Noah land surface model advances in the National Centers for Environmental Prediction operational mesoscale Eta model, *Journal of Geophysical Research*, 108, D22, 8851, doi:10.1029/2002 JD003296

Emanuel, K. A., 1989. Dynamical theories of tropical convection, *Aust. Meteor. Mag.,* 37, 3–10.

Emanuel, K., Desautels C., Holloway C., and Korty R., 2004. Environmental control of tropical cyclone intensity, *Journal of the Atmospheric Sciences*, 61, 843-857.

Frank, W. M., and Ritchie E. A., 1998. Effects of environmental flow upon tropical cyclone structure, *Monthly Weather Review,* 127, 2044 -2061.

Ge, X., Li T., and Peng M., 2013. Effects of Vertical Shears and Midlevel Dry Air on Tropical Cyclone Developments, *J. Atmos. Sci*., 70, 3859–3875, doi:10.1175/JAS-D-13-066.1.

Hasan, M. A., and Islam A.K.M.S., 2018. Evaluation of Microphysics and Cumulus Schemes of WRF for Forecasting of Heavy Monsoon Rainfall over the Southeastern Hilly Region of Bangladesh, *Pure Appl. Geophys,* https://doi.org/10.1007/s00024-018-1876-z.

Hill, K. A., and Lackmann G. M., 2009. Influence of environmental humidity on tropical cyclone size, *Monthly Weather Review*, 137, 3294 -3315.

Hong and Lim., 2006. A new vertical discussion package with an explicit treatment of entrainment processes. *Mon. Wea. Rev.,* 132, 2318-2240.

Hong, S. Y., J. Dudhia and S. H. Chen., 2004. A revised approach to ice microphysical processes for the bulk parameterization of clouds and precipitation, *Mon. Wea. Rev.,* 132, 103-120.

Kain, J. S., and J. M. Fritsch., 1990. A one-dimensional entraining/detraining plume model and its application in convective parameterization. *J. Atmos. Sci.,* 47, 2784-2802.

Kaplan, J., DeMaria M., and Knaff J. A., 2010. A Revised Tropical Cyclone Rapid Intensification Index for the Atlantic and Eastern North Pacific Basins, *Weather Forecast.,* 25, 220–241, doi:10.1175/2009 WAF2222280.1.

Kimball, S. K., 2006. A Modeling Study of Hurricane Landfall in a Dry Environment, *Mon. Weather Rev*., 134, 1901–1918, doi:10.1175/MWR3155.1.

Larissa E. B., and Christopher S. B., 2005.The relationship between wind Speed and precipitation in the Pacific ITCZ, *Atmospheric Sciences,* 18, 4317-4328.

Mansell, S. Y., and S. H. Chen., 2010. A revised approach to ice microphysical processes for the bulk parameterization of clouds and precipitation, *Mon. Wea. Rev.,* 152, 105-120.

Mlawer, E. J., Tubman S. J., Brown P. D., Lacono M. J., and Clough S. A., 1997. Radiative transfer for inhomogeneous atmosphere: RRTM, a validated correlated-k model for the longwave, *J. Geophys. Res.,* 102, D14, 16663-16682.

Tao, D., and Zhang F., 2014. Effect of environmental shear, Sea surface temperature, and ambient moisture on the formation and predictability of tropical cyclones: An ensemble mean perspective, *J. Adv. Model*. Earth Syst., 6, 384–404, doi:10.1002/2014MS 000314.

Taraphdar, S., Mukhopadhyay P., Leung L. R., Zhang F., Abhilash S., and Goswami B. N., 2014. The role of moist processes in the intrinsic predictability of Indian Ocean cyclones, J. *Geophys. Res. Atmos.,* 119, 8032–8048.

Wang, Z., Montgomery M. T., and Dunkerton T. J., 2009. A dynamically based method for forecasting tropical cyclogenesis location in the Atlantic sector using global model products, Geophys. Res. Lett., 36, L03801, doi:10.1029/2008GL035586.

Wu, L., Su H., Fovell R. G., Dunkerton T. J., Wang Z., and Kahn B. H., 2015. Impact of environmental moisture on tropical cyclone intensification*, Atmos. Chem. Phys*., 15, 14041–14053.

Wu, W., and Chen J. L., 2012. Sensitivity of tropical cyclone precipitation to atmospheric moisture content: Case study of Bilis (2006), *Atmos. Oceanic Sci. Lett*., 5, 420–425.

Ying, Y., and Zhang Q., 2012. A Modeling Study on Tropical Cyclone Structural Changes in Response to Ambient Moisture Variations, *J. Meteorol. Soc. Jpn*., 90, 755–770, doi:10.2151/jmsj.2012-512.